ELSEVIER Nuclear Instruments and Methods in Physics Research B 146 (1998) 285–289

NIM B
Beam Interactions with Materials & Atoms

TEM observations of iron and nickel foils irradiated by MeV fullerenes at room temperature ☆

H. Dammak [a], A. Dunlop [b,*]

[a] *Laboratoire CPS, CNRS URA 453, Ecole Centrale Paris, Grande Voie des Vignes, 92295 Chatenay-Malabry, France*
[b] *Laboratoire des Solides Irradiés, S.E.S.I., CEA/Ecole Polytechnique, 91128 Palaiseau Cedex, France*

Abstract

It is shown that a new specific effect takes place in iron during irradiation with ~10 MeV fullerene beams. A dislocation line with various shapes is observed in the close vicinity of the projectile path leading to a strain field confined inside a 20–40 nm diameter "cylinder". Similarly to previous observations in titanium and zirconium (Dammak et al., Phys. Rev. Lett. 74 (1995) 1135), this effect might be due to the strong localisation of the energy deposited during the projectile slowing-down process. However no damage is observable in nickel irradiated in the same conditions. These results should be explained by the previously established relation between the sensitivity of a metal to a high rate of energy deposition in electronic excitations and the existence of a high pressure phase in the pressure-temperature phase diagram (Dammak et al., Nucl. Instr. and Meth. B 107 (1996) 204).

1. Introduction

Since 1989, it has been established that high rates of linear energy deposition in *electronic processes* (LET) during swift heavy ion irradiations (typically GeV Ar to U ions) can induce in iron either a partial recombination of the defects created by elastic collisions or an additional point defect creation [1–3]. For a sufficiently high LET level (>40 keV/nm), the second effect becomes predominant. However these defects created in the close vicinity of the ion path are isolated point defects, so that they are not observable by transmission electron microscopy (TEM). Their formation was deduced from the analysis of in situ electrical resistivity measurements during low temperature irradiations [3]. On the other hand, in nickel only a partial recombination of the defects created by elastic collisions was evidenced [4], so that if a LET level threshold for additional defect creation by electronic processes does exist it should be higher than 75 keV/nm.

It has been recently established that during the slowing-down of energetic cluster ions (typically 10–40 MeV C_{60} or Au_4 projectiles) the LET levels are similar or higher than those obtained during GeV monoatomic ion irradiations. Moreover it was pointed out that the resulting structural

☆ Irradiations were performed on the tandem accelerator, IPN Orsay (France).

* Corresponding author. Fax: +33 01 6933 3022; e-mail: annie.dunlop@polytechnique.fr

0168-583X/98/$ – see front matter
PII: S0168-583X(98)00520-5

modifications were extremely important, due to the very strong localisation of the deposited energy. In titanium, GeV U ions create an alignment of 3–5 nm width dislocation loops, but 18 MeV C_{60} ions create quasi-continuous tracks of about 20 nm diameter [5]. It thus seemed natural to bombard iron and nickel targets with a few 10 MeV C_{60} ions in order to search for much stronger damaging effects.

2. Experimental results

Pure iron and nickel polycrystalline targets, electrochemically thinned for TEM observations (i.e. thickness ~100 nm), have been irradiated at 300 K with a few 10 MeV C_{60} at different fluences (Table 1).

2.1. Nickel

TEM observations show that no damage is observable by TEM in nickel irradiated with 40 MeV C_{60} ions (highest energy available in the Tandem accelerator) for which the LET level is of about 93 keV/nm at the target entrance.

2.2. Iron

In iron, after low fluence irradiations, TEM observations show tracks with a density close to the impinging ion fluence. Fig. 1(a) and (b) show typical images of tracks obtained after irradiations with 20 and 31 MeV C_{60} at fluences of a few 10^9 ions/cm^2. From numerous observations, we noticed that the contrast of tracks varies strongly with the diffraction conditions. A track is essentially formed by a dislocation line which can exhibit several shapes: i) two quasi-parallel lines joined at the ends, i.e. near the surfaces (Fig. 3), ii) one line separated into two lines joined at the end (Fig. 2), and iii) more complicated structures. We also noticed that the shape of the dislocation lines seems to vary with the crystallographic orientation of the grain in respect to the ion beam direction.

On the other hand, when the tracks are imaged with particular diffraction conditions (i.e. two beam conditions using $\mathbf{g} = (1\,1\,0)$ which is almost perpendicular to the track), fringes perpendicular to the ion path are observed in addition to the dislocation lines. Examples are shown in Fig. 2 after 20 and 40 MeV C_{60} irradiations: the dislocation lines appear as white contrasts going through the fringes. From the length of the fringes one can estimate a track diameter as the extension of the strain field around the ion path. Fig. 2 shows that the track diameter increases as the C_{60} ion energy is increased (i.e. as the LET level increased). The "diameters" reported in Table 1 were determined in this way (as we did not observe

Table 1
Characteristics of the experiments presented in this paper

Incident energy (MeV)	C_{60} ion fluence (cm^{-2})	Average LET (keV/nm)	Projected range R_p (nm)	Average displaced atoms/i.d.	TEM observations	Track diameter (nm)
Fe						
18	3×10^9	52	328	~17	Tracks	16–21
20	3×10^9	56	357	~16	Tracks	16–22
31	5.3×10^9	76	484	~13	Tracks	
	1.7×10^{11}	76	484		Tracks and dense dislocation lines	
40	2.6×10^9	91	584	~9	Tracks	30–45
Ni						
40	3×10^9	86	569	~10	No observable damage	

Averaged LET levels and numbers of displaced atoms per interatomic distance were calculated for the first 100 nm of the projected range (i.e. target thickness).

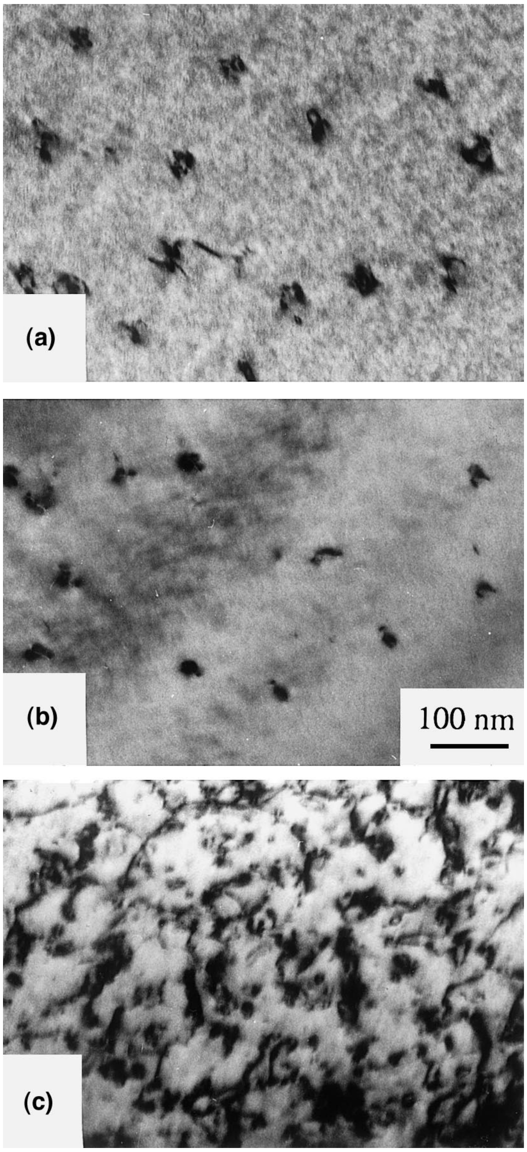

Fig. 1. Bright field images of iron irradiated at 300 K: (a) with 31 MeV C_{60} ions up to 5.3×10^9 cm^{-2}, (b) with 20 MeV C_{60} ions up to 3×10^9 cm^{-2} and (c) with 31 MeV C_{60} ions up to 1.7×10^{11} cm^{-2}. The electron beam direction is parallel to the ion beam. In (b) the incident ion direction is parallel to [0 0 1]. (c) shows dislocation lines due to the partial track overlapping and impacts of non overlapped tracks.

tracks induced by 30 MeV projectiles in these very particular diffraction conditions, no diameter for this energy could be reported in the table). These

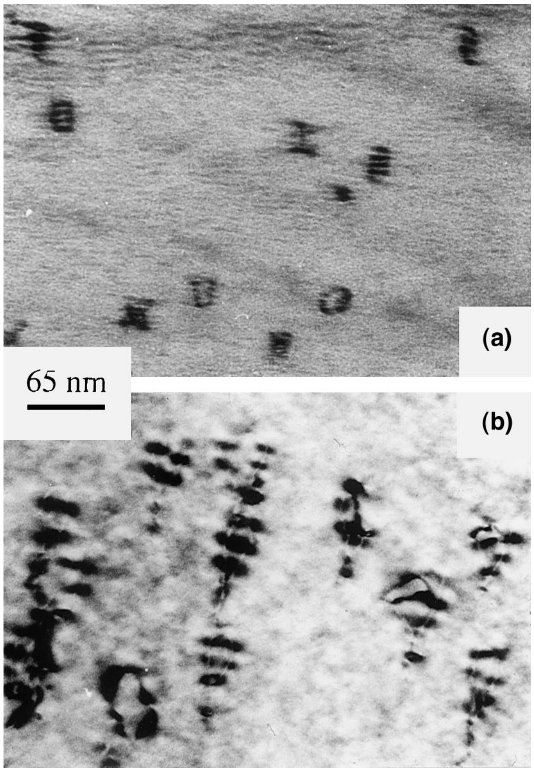

Fig. 2. Bright field images of iron irradiated at 300 K: (a) with 20 MeV C_{60} ions up to 3×10^9 cm^{-2} and (b) with 40 MeV C_{60} ions up to 2.6×10^9 cm^{-2}. The sample is tilted in the microscope by 36° and 40° for (a) and (b), respectively. The thicknesses in the selected areas are different, so that corresponding tracks lengths are different for (a) and (b).

diameters are very close to those measured for tracks obtained in titanium and zirconium irradiated in the same conditions [5].

Fig. 1(c) shows a bright field image of an iron sample irradiated with 31 MeV C_{60} ions at a fluence of 1.7×10^{11} cm^{-2}. The image shows a dense network of dislocation lines and isolated tracks. The density of the observed tracks is about 5×10^{10} cm^{-2} which is three times lower than the ion fluence. During this high fluence irradiation, there is a significant spatial overlap of the tracks. In fact the ion fluence threshold above which tracks begin to overlap is equal to the inverse of the track cross section area (about 10^{11} ions cm^{-2}).

The determination of the tracks Burgers vectors is not easy due to the limitation of the tilt angle in

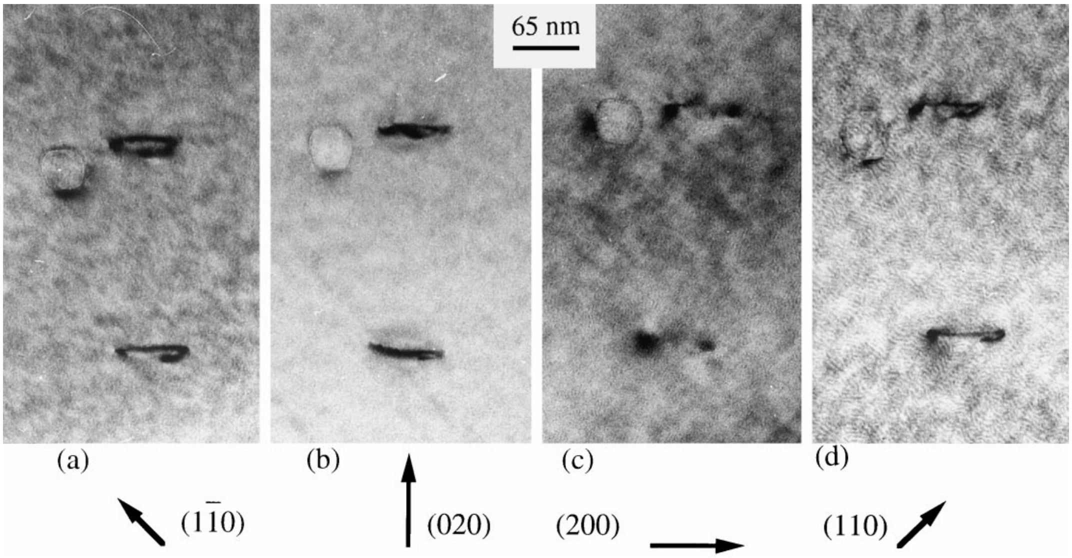

Fig. 3. Bright field images of iron irradiated at 300 K with 31 MeV C_{60} ions. The sample is tilted in the microscope. Observations in two beam conditions with $\mathbf{g} = (1\,\bar{1}\,0)$, (020), (200) and (110) from the left to the right, respectively. The dislocation extinction is obtained with $\mathbf{g} = (200)$.

the electron microscope. Fig. 3 shows various bright field images of a track obtained using different two beam conditions. With $\mathbf{g} = (200)$, the dislocation line is extinct and only a black-white contrast at the ends is observed. The track Burgers vector is perpendicular to (200) and should thus be a combination of the two vectors $\mathbf{b}_1 = 1/2\,[0\,1\,1]$ and $\mathbf{b}_2 = 1/2\,[0\,1\,0]$, which were previously observed in Ref. [6].

3. Discussion and conclusion

The linear rates of energy deposition in both electronic processes and elastic collisions for C_{60} ions is calculated as the sum of the energy losses of 60 individual carbon atoms. As a matter of fact, all available experimental determinations of energy losses during cluster irradiations [7–9] agree with this additive rule within experimental uncertainties. At 30 MeV the rate of energy deposition in elastic collisions is 30 times lower than that for inelastic collisions. The number of displaced atoms in elastic processes evaluated using the TRIM code [10] is of about 10 every interatomic distance (i.d.) and decreases as the C_{60} energy increases (Table 1). On the other hand the radial range of primary target atoms ejected in elastic collisions is of some 10 nm. If the observed damage was only due to elastic collisions then (i) the created damage should decrease when the C_{60} energy increases and (ii) the created defects should agglomerate in several dislocation loops far from the ion path [11]. At the opposite, TEM observations show that the damage creation at 40 MeV is *stronger* than that at 20 MeV and is located in the *close vicinity* of the ion path. *Dislocation lines thus result from high energy deposition in electronic excitations.*

As mentioned in the introduction, similar LET levels can be obtained using GeV monoatomic projectiles (up to 70 keV/nm using GeV uranium ions, 50–90 keV/nm with C_{60} cluster ions), but then only isolated point defects are generated [3]. The explanation for such different behaviours might originate from the great difference in the velocities of swift heavy ions and C_{60} projectiles. The transport of energy away the ion path is governed by the ejected δ electrons, which have angular and kinetic energy distributions related to the projectile velocity. The volume in which the energy is deposited is related to the radial range of secondary electrons. The lower the projectile velocity, the higher the deposited energy density and thus the space charge density. Using GeV Pb or U ions the radial range of δ electrons is of some 1000 nm, whereas using a few 10 MeV C_{60} ions, this radial range falls to a few interatomic distances. In this latter case, the deposited energy density can reach values as high as 100 eV/atom. The relaxation of such a high energy density induces the formation of the observed dislocations and strain fields around the ion path.

The sensitivity of metals to high LET levels was previously related to the existence of a high pressure phase in the phase diagram of metals [12]. Titanium, zirconium and iron are metals in which (i) a high pressure phase exists in the pressure–temperature phase diagram [13,14] and (ii) high levels of linear energy deposition in electronic excitations during GeV Pb or U ion irradiations induce either additional point defect creation or latent track formation [4,12] Moreover, an enhancement of the damage creation is obtained following $\sim$10 MeV C_{60} ions irradiations of these metals due to the high deposited energy density ([5], this work). But such high energy density is not sufficient to induce any structural damage observable by TEM in a nickel target, which could be explained by the absence of a phase transformation at high pressure in the phase diagram of nickel.

Acknowledgements

We are very grateful to Serge Della-Negra, IPN/Orsay for delivering the fullerene beams.

References

[1] A. Dunlop, D. Lesueur, J. Dural, Nucl. Instr. and Meth. B 42 (1989) 182.
[2] A. Dunlop, D. Lesueur, J. Morillo, J. DuraL, R. Spohr, J. Vetter, Nucl. Instr. and Meth. B 48 (1990) 419.
[3] A. Dunlop, D. Lesueur, P. Legrand, H. Dammak, Nucl. Instr. and Meth. B 90 (1994) 330.
[4] A. Dunlop, D. Lesueur, Radiat. Eff. and Def. in Solids 126 (1993) 123.
[5] H. Dammak, A. Dunlop, D. Lesueur, A. Brunelle, S. Della-Negra, Y. Le Beyec, Phys. Rev. Lett. 74 (1995) 1135.
[6] B.L. Eyre, R. Bullough, Phil. Mag. 12 (1965) 31.
[7] K. Baudin, A. Brunelle, M. Chabot, S. Della-Negra, J. Depauw, D. Gardes, P. Hakansson, Y. Le Beyec, A. Billebaud, M. Fallavier, J. Remillieux, J.C. Poizat, J.P. Thomas, Nucl. Instr. Meth. B 94 (1994) 341.
[8] C. Tomaschko, D. Brandl, R. Krüger, M. Schurr, H. Voit, Nucl. Instr. Meth. B 103 (1995) 407.
[9] D. Ben-Hamu, A. Baer, H. Feldman, J. Levin, O. Heber, Z. Amitay, Z. Vager, D. Zajfman, Phys. Rev. A 56 (1997) 4786.
[10] J.P. Biersack, L.G. Haggmark, Nucl. Instr. and Meth. 174 (1980) 257.
[11] B.C. Master, Phil. Mag. 11 (1964) 881.
[12] H. Dammak, A. Dunlop, D. Lesueur, Nucl. Instr. and Meth. B 107 (1996) 204.
[13] S.K. Sikka, Y.K. Vohra, R. Chidambaram, Prog. Mater. Sci. 27 (1982) 245.
[14] P.M. Giles, M.H. Longenbach, A.R. Marder, J. Appl. Phys. 42 (1971) 4290.